IOP Conference Series: Materials Science and Engineering

PAPER • OPEN ACCESS

Compressed rectangular plates stability beyond the elastic limit

To cite this article: T Mavlonov *et al* 2020 *IOP Conf. Ser.: Mater. Sci. Eng.* **883** 012199

View the article online for updates and enhancements.

This content was downloaded from IP address 213.230.109.7 on 21/07/2020 at 10:20

IOP Conf. Series: Materials Science and Engineering **883** (2020) 012199 doi:10.1088/1757-899X/883/1/012199

Compressed rectangular plates stability beyond the elastic limit

T Mavlonov[1]*, B Yuldoshev[1], K Ismayilov[2] and S Toshev[2]

[1]Tashkent Institute of Irrigation and Agricultural Mechanization Engineers, Tashkent, Uzbekistan
[2]Samarkand State Architecture and Civil Engineering Institute, Samarkand, Uzbekistan

baxtiyor_yuldashev68@mail.ru

Abstract. The paper provides a detailed analysis of the methods for calculating the thin-walled structure stability under static and dynamic loads, and the results of well-known studies related to assessing the stability of thin-walled structures. The paper gives a methodology for assessing the thin-walled structure stability and the analysis of stability loss of rectangular plates beyond the elasticity of the material. The stability loss of rectangular plates beyond the elastic limit of the material is investigated in the paper. A formula is proposed for determining the longitudinal forces in a plate under a state of infinitely small bending. An analytical formula is given to assess stability for the case of a hinged supported rectangular plate compressed in two directions beyond the elastic limit at various widths (b)-thickness (h) ratios of the plate. The proposed diagram of the plate material strain is in good agreement with the Berlin – Dahlem experimental diagram. It was stated that under linear hardening of the material, a square plate of flexibility $b/h \geq 20$, loses its stability within the yield strength. Beyond the yield strength, flexibility $b/h < 5$ corresponds to stability loss.

1. Introduction

Theoretical and experimental studies of thin-walled structure stability are investigated in detail in [1–5]. The behavior after convexity of rectangular orthotropic multilayer composite plates with initial defects under shear stress in a plane was studied in [6]. Using form functions of the Timoshenko type for the initial bifurcation analysis of stability loss and subsequent studies of the post-slip type, analytical solutions were obtained in closed form for the stability loss loads and the variable states after buckling. Moreover, the considered plates were assumed to be infinitely long in the longitudinal direction.

The closed analytical expressions for calculating the effective width of thin plates under inhomogeneous plane loading were presented in [7]. It was assumed that the longitudinal edges are the straight lines and can move freely in the plate plane. The proposed expressions were very useful for calculating the limiting state of thin I-section beam columns or channel sections under general types of load. They allow designers to calculate the effective section width using simple formulas that are suitable for manual calculation and avoid the costs and efforts that may be required for any numerical non-linear analysis.

The bending behavior of a biaxially compressed orthotropic double-layer graphene sheet (DLGS) embedded in an elastic medium was studied based on the theory of nonlocal elasticity. DLGS is

Content from this work may be used under the terms of the Creative Commons Attribution 3.0 licence. Any further distribution of this work must maintain attribution to the author(s) and the title of the work, journal citation and DOI.
Published under licence by IOP Publishing Ltd

modeled as a nonlocal double-layer plate, which contains the effect of small scale and van der Waals interaction forces. The van der Waals interaction between graphene layers is modeled as a set of linear springs using the Lennard-Jones potential model. Using the principle of virtual work, the equilibrium equations are derived on the basis of the theory of shear strains of the first order and the Eringen nonlocal differential defining relations [8].

The researchers in [9] described a deep study of mathematical and computational programs in developing an effective design methodology based on modeling using the finite element method. This methodology suits the applications in the practical construction of structural components used in the manufacturing of complex lightweight RTM-type composites and covers thick and thin shell-type composites.

An analysis of the stability loss of orthotropic nanoplates, such as graphene, using the theory of refined plates with two variables and nonlocal small-scale effects was presented in [10]. The theory of a refined plate with two variables takes into account the effects of transverse shear and the parabolic distribution of transverse shear strain along the plate thickness, so there is no need to use correction coefficients of shear. Nonlocal constitutive equations of motion for monolayer graphene are derived from the principle of virtual displacements. A closed-shape solution for bending loads on a simply supported rectangular orthotropic nanoplate subjected to plane loading was obtained using the Navier method. The numerical results obtained with the present theory are compared with the first-order shear strain theory for various correction coefficients of shear. It was proved that the dimensionless loss of stability of an orthotropic nanoplate is always less than that of an isotropic nanoplate.

The study in [11] is related to modeling and analysis for a dense safety valve, thus successfully applying a systematic method for the design and analysis of similar valves. The aim of the work is to solve two important problems: one concerns the positions of the control valve, influenced by the flow force, and the other concerns the opening of the safety valve controlled by a thin annular plate. Computational Fluid Dynamics method (CFD) is used to represent the flow strength. Using a series of experiments, the dependence of flow rate on pressure drop shows the rationality of CFD results. To obtain the opening of the safety valve with higher accuracy, the theory of large deflection of thin plates is applied.

Various influential factors, such as element size, defining relations, second-order structure effects, and membrane effects in the loss of stability region have been discussed to achieve better validation using experimental data. As the load increases, plastic strain in the U-shaped rib near the end stiffening rib gradually increases under the influence of initial defects and stress concentration [12].

The limit bending strength of bisymmetric and monosymmetric I-beams subjected to local bending in the bridges was investigated using nonlinear finite element analysis, including post-bending behavior. Plate trusses made of high strength steel (HPS) and ordinary steel were modeled three-dimensionally with thin shell elements, and limit strength analysis was performed using universal non-linear methods provided by commercially developed finite element analysis (FEA), software ABAQUS. Elastic-plastic strain hardening was considered as the fundamental correlation for both HPS and ordinary steel, and the initial drawbacks were taken into account, and the residual stresses were superimposed on the hypothetical built-up areas [13].

In [14], a theoretical solution to the plane contact problem of the theory of elasticity is presented, based on the method for determining the convergence of elastic bodies using an elastic model of half-space; on its basis the contact strain (change in diameter) of circular cylinders with parallel axes was determined. The possibility of obtaining an exact solution to the problem using an elastic half-spatial model based on the Hertz theory was shown for the first time. It was shown that the well-known Kowalski solution for contact strain of circular cylinders with parallel axes is a rough approximation of a more accurate solution to the problem. It was established that the result is in good agreement with the experimental data of Dinnik.

In [15], the long-term stability of plates and shells of polymer materials was considered taking into account their economic properties. The problems of long-term stability of plates and shells made of polymer materials were discussed in a review report presented by Yu.N.Rabotnov.

Along with this, stability assessment, dynamic behavior, and wave phenomena in various thin-walled structures were studied in [16–22]. These are just some of the works dedicated to the subject of this paper.

The above review of published works shows that the stability assessment under static and dynamic loads is differently conducted in different studies, and each theory or method used has its advantages and disadvantages.

2. Methods

The rational use of plates in various fields of construction and mechanical engineering requires the development of an updated methodology for calculating the stability of plates taking into account the peculiarities of their mechanical properties.

As is known, at the bifurcation of plane equilibrium state of a compressed plate to a bending state its stress-strain state changes substantially.

Let us present the geometrical relations [1] connecting strains with displacements in the case when the surface of the plate is curved downward

$$\Delta\chi_x = -\frac{\partial^2 \Delta w}{\partial x^2}; \qquad \Delta\chi_y = -\frac{\partial^2 \Delta w}{\partial y^2}; \qquad \Delta\chi_{xy} = -2\frac{\partial^2 \Delta w}{\partial x \partial y} \tag{1}$$

where $\Delta\chi_x, \Delta\chi_y$ are the bending strain; $\Delta\chi_{xy}$ is torsion strain; $\Delta w(x, y)$ is deflection function.

According to the theory of small elastic-plastic strains [2], stresses $\Delta\sigma_x; \Delta\sigma_y; \Delta\tau_{xy}$ are related to strains by the following relations

$$\Delta\sigma_x = \frac{4}{3}\psi\left(\Delta\chi_x + \frac{1}{2}\Delta\chi_y\right)z; \qquad \Delta\sigma_y = \frac{4}{3}\psi\left(\Delta\chi_y + \frac{1}{2}\Delta\chi_x\right)z \tag{2}$$

$$\Delta\tau_{xy} = \frac{1}{3}\psi\Delta\chi_{xy}z. \qquad \psi = \frac{\sigma_i}{\xi_i} \tag{3}$$

The plate material is assumed to be incompressible and $\Delta\varepsilon_0 = 0, \ \Delta\sigma_z = 0$

We believe that the infinitely small bending of a rectangular plate occurs as a result of the bifurcation of its equilibrium state: in this case, the plate passes from a flat form of equilibrium to a bending one (figure 1, a). The secant module at which bifurcation occurs, we denote by ψ_0 , the point M_0 on the diagram $\sigma - \varepsilon$ corresponds to this module. There are three types of stresses and strains. Therefore, there are three formulas for the secant module ψ [3]:

$$\psi_x = \psi_0\left[1 + \frac{4}{3}\frac{\left(\Delta\chi_x + 0,5\Delta\chi_y\right)}{\varepsilon_0}z\left(1 - \frac{E_k}{\psi_0}\right)\right]$$

$$\psi_y = \psi_0\left[1 + \frac{4}{3}\frac{\left(\Delta\chi_y + 0,5\Delta\chi_x\right)}{\varepsilon_0}z\left(1 - \frac{E_k}{\psi_0}\right)\right] \tag{4}$$

$$\psi_{xy} = \psi_0\left[1 + \frac{1}{3}\frac{\left(\Delta\chi_{xy}\right)}{\varepsilon_0}z\left(1 - \frac{E_k}{\psi_0}\right)\right]$$

These formulas show that in the upper half of the thickness of plate section, secant moduli, in comparison with the value of ψ_0, decrease $(z > 0)$;

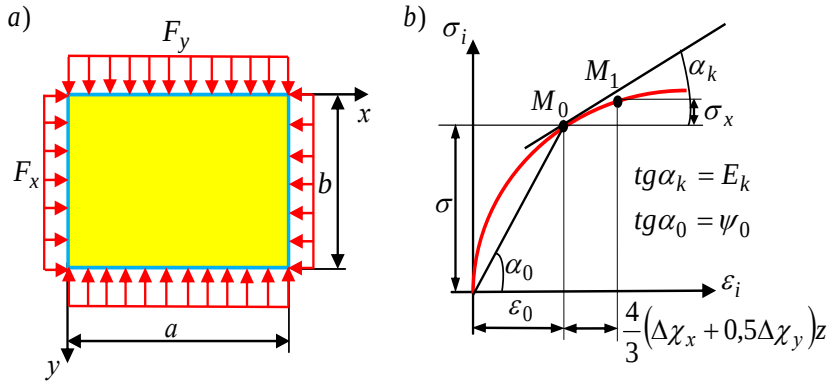

Figure 1. Design scheme and diagram of the material strain.

Consider the stress state of a rectangular plate, compressed in two directions. In this case, the condition is satisfied:

$$\sigma_x = F_x; \quad \sigma_y = F_y; \quad \sigma_z = 0; \quad \tau_{xy} = 0 \tag{5}$$

where $F_x; F_y$ are the compressive conditions in the directions X *and* Y, respectively.

In this case, the strains $\varepsilon_x; \varepsilon_y; \varepsilon_z$ are nonzero, and the strains along the vertical axis z are found from the condition of the material incompressibility $\varepsilon_x + \varepsilon_y + \varepsilon_z = 0$; $\varepsilon_x = -(\varepsilon_y + \varepsilon_z)$.

Since the stresses σ_x, σ_y are set, the value of the secant module $\psi = \dfrac{\sigma_i}{\varepsilon_i}$ can be found. To do this, at the beginning we calculate

$$\sigma_i = \sqrt{\sigma_x^2 - \sigma_x\sigma_y + \sigma_y^2} = \sqrt{F_x^2 - F_xF_y + F_y^2}; \; \sigma_i = F_x\sqrt{1-\alpha+\alpha^2}; \qquad \alpha = \frac{F_y}{F_x} \tag{6}$$

Knowing the stress intensity, we determine the strain intensity ε_i based on the adopted diagram $\sigma_i - \varepsilon_i$, which allows us to establish the dependencies $\sigma_i = \Phi(\varepsilon_i)$. Next, we find the secant moduli $\varepsilon_x, \varepsilon_y$ using the formula $\psi = \Phi(\varepsilon_i)/\varepsilon_i$. Using this formula, the strains are calculated when deriving the relations connecting the forces and moments with the strains, here we will proceed from the assumption that the strains lie beyond the limits of Hooke's law.

The longitudinal forces in the plate, which is in the state of infinitely small bending, are determined by relations:

$$N_x = \frac{4}{3}(\varepsilon_x + 0.5\varepsilon_y)\psi_0 h - \frac{4}{3}\frac{(\Delta\chi_x + 0.5\Delta\chi_y)^2}{\varepsilon_0}\left(1 - \frac{E_k}{\psi_0}\right)D_0$$

$$N_y = \frac{4}{3}(\varepsilon_y + 0.5\varepsilon_x)\psi_0 h - \frac{4}{3}\frac{(\Delta\chi_y + 0.5\Delta\chi_x)^2}{\varepsilon_0}\left(1 - \frac{E_k}{\psi_0}\right)D_0 \tag{7}$$

$$\Delta S = -\frac{1}{12}\frac{(\Delta\chi_{xy})^2}{\varepsilon_0}\left(1 - \frac{E_k}{\psi_0}\right)D_0. \quad D_0 = \frac{4}{3}\psi_0 I_y = \frac{1}{9}\psi_0 h^3$$

Considering that $4(\varepsilon_x + 0{,}5\varepsilon_y)\psi_0 = 3F_x$; $4(\varepsilon_y + 0{,}5\varepsilon_x)\psi_0 = 3F_y$ and neglecting in the formulas (7) the values of the second-order of smallness, we find:

$$N_x = hP_x;\ N_y = hP_y;\ S = 0. \tag{8}$$

We write expressions for infinitely small bending and torques

$$\Delta M_x = -\left(\Delta\chi_x + 0.5\Delta\chi_y\right)\left[1 - \frac{4}{3}\frac{\left(\varepsilon_x + 0.5\varepsilon_y\right)}{\varepsilon_0}\left(1 - \frac{E_k}{\psi_0}\right)\right]D_0$$

$$\Delta M_y = -\left(\Delta\chi_y + 0.5\Delta\chi_x\right)\left[1 - \frac{4}{3}\frac{\left(\varepsilon_y + 0.5\varepsilon_x\right)}{\varepsilon_0}\left(1 - \frac{E_k}{\psi_0}\right)\right]D_0 \tag{9}$$

$$\Delta H = -\frac{1}{4}\Delta\chi_{xy}D_0$$

Equations (9) are reduced to a homogeneous equation with respect to the deflection function $w(x, y)$; for this purpose, the equilibrium equation is used, in which the vertical load on the element is represented by the projections of compressive stresses F_x; F_y on the axis z:

$$\frac{\partial^2 \Delta M_x}{\partial x^2} + 2\frac{\partial^2 \Delta H}{\partial x \partial y} + \frac{\partial^2 \Delta M_y}{\partial y^2} = \left(-F_x\frac{\partial^2 w}{\partial x^2} - F_y\frac{\partial^2 w}{\partial y^2}\right)h \tag{10}$$

Introducing strain expressions (9) through the deflection function (1), we obtain the stability equation of a rectangular plate, compressed in two directions; beyond the elastic limits it can be written in a simpler form:

$$\nabla^2\nabla^2 w - \left[\frac{\partial^4 w}{\partial x^4} + \frac{1}{2}\frac{\partial^4 w}{\partial x^2 \partial y^2}\right]\frac{4}{3}\frac{\xi_x + 0,5\xi_y}{\xi_0}\left(1 - \frac{E_k}{\psi_0}\right) -$$
$$-\left[\frac{\partial^4 w}{\partial y^4} + \frac{1}{2}\frac{\partial^4 w}{\partial x^2 \partial y^2}\right]\frac{4}{3}\frac{\xi_y + 0,5\xi_x}{\xi_0}\left(1 - \frac{E_k}{\psi_0}\right) = \tag{11}$$
$$= -\frac{h}{D_0}\left(P_x\frac{\partial^2 w}{\partial x^2} + P_y\frac{\partial^2 w}{\partial y^2}\right)$$

In the case of a hinged-supported rectangular plate compressed in two directions, beyond the elastic limits, the deflection function can be represented as the product of sines

$$w(x, y) = C_{m1}\sin\frac{m\pi x}{a}\sin\frac{\pi y}{b} \tag{12}$$

This function corresponds to the case when a rectangular plate with sides a and b loses stability along one half-wave along the axis y, and along m half-waves along the axis x.

The deflection function (12) satisfies the boundary conditions according to which the deflections and bending moments should vanish along the contour of the plate.

Substituting the function (12) into (11) we obtain the stability equation for the hinged-supported plate, for the geometrical parameter of the plate b/h;

$$\frac{b^2}{h^2} = \frac{\pi^2\psi_0}{9F_x}\frac{\left(1 + m^2t^2\right)^2 - \left[m^2\left(m^2t^4 + \frac{t^2}{2}\right) + \left(1 + \frac{m^2t^2}{2}\right)\alpha\right]}{\left(m^2t^2 + \alpha\right)\sqrt{1 - \alpha + \alpha^2}}\left(1 - \frac{E_k}{\psi_0}\right) \tag{13}$$

To construct the necessary graphs reflecting the plate stability, relations (13) are used.

A group of equations related to the parameter $\alpha = P_y / P_x = 1/2$ and a group of equations related to the parameters $\alpha = P_y / P_x = 1/4$ that connect the flexibility of the plate b/h with some critical points M_0 in the diagram $\sigma_i - \varepsilon_i$ are obtained. To each point M_0 taken on the diagram corresponds to the flexibility of the plate b/h.

Choosing such a point, we have the value of secant modulus $\psi_0 = \sigma_i / \varepsilon_i$ and the value of tangent modulus $E_k = d\sigma_i / d\varepsilon_i$.

The load parameter F_x, which is in the denominator of the right-hand sides of the above equations is expressed in terms of the stress intensity σ_i by formula (6).

Therefore, the quotient ψ_{0i} / F_x, located on the right-hand sides of the stability equations (13) at $(\alpha = 1;\ \alpha = 0.5;\ \alpha = 0.25;\ \alpha = 0)$ is replaced by the following expression

$$\frac{\psi_0}{P_x} = \frac{\sigma_i}{\varepsilon_i} \frac{\sqrt{1-\alpha+\alpha^2}}{\sigma_i} = \frac{\sqrt{1-\alpha+\alpha^2}}{\varepsilon_i}. \tag{14}$$

3. Results

Repeated short-term operation of the equipment is used for step-by-step control of the supply by switch in on and off the pump electric motors. Non-uniform pump operation is characterized by the condition that the pump supply is equal to the corresponding water consumption at any time.

Thus, for any point M_0 in the compression diagram $\sigma_i - \varepsilon_i$, the right-hand side of each of these equations becomes a known number that determines the flexibility of the plate b/h.

The proposed compression diagram $\frac{\sigma_{vr} - \sigma_i}{\sigma_{vr} - \sigma_T} = \left(\frac{\varepsilon_{vr} - \varepsilon_i}{\varepsilon_{vr} - \varepsilon_T} \right)^n$ is in good agreement with the experimental diagram obtained in classical experiments in Berlin-Dalem laboratory. Therefore, the numerical results obtained in the paper relating to the stability of a compressed hinged-supported rectangular plate can be considered quite reliable.

Figures 2 and 3 show graphs of plate flexibility b/h versus stress intensity σ_i and strain rate ε_i for a square steel plate, the material of which is endowed with a linear hardening diagram.

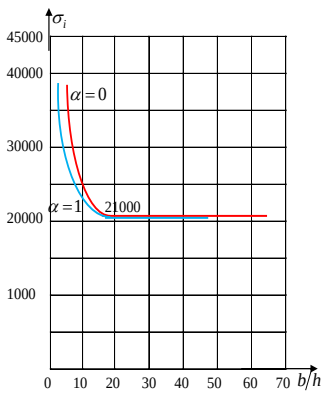

Figure 2. Change in stress intensity depending on *b\h*

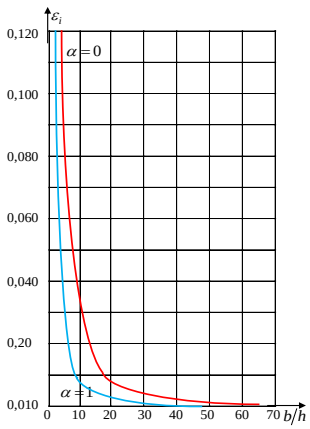

Figure 3. Change in strain intensity depending on *b\h*

4. Conclusions

1. A material strain diagram was proposed which is in good agreement with the experimental Berlin – Dalem diagram.

2. It was established that under linear hardening of the material, a square plate with flexibility $b/h \geq 20$ loses stability under compressive stresses slightly different from the yield strength of the material $\sigma_T = 21000\, N/sm^2$.

3. Under compressive stresses of about $30000\, Nm^2$ and higher, and at plate flexibility of $b/h < 5$ the issues of stability of such plates should be considered according to the theory of thick plates.

4. It was stated that under infinite bending of the compressed plate beyond the elastic limit, the secant modulus of its longitudinal fibers decreases (as in the reloading zone), and in the unloading zone, it moves along an infinitesimal small section which is tangent to the critical point in the compression diagram $\sigma_i - \varepsilon_i$. In this case, the secant modulus in the reloading zone decreases, and in the unloading zone it increases.

References

[1] Ilyushin A A 1963 Plasticity. Fundamentals of the general mathematical theory *Publishing House of the Academy of Sciences of the USSR* (Moscow)
[2] Volmir A S 1963 Stability of elastic systems (Moscow Fizmatgiz)
[3] Zubchaninov V G 1964 On the theory of stability of plates beyond the elastic limit *USSR Acad Sci MTT* **4** pp 11–15
[4] Krasnikov N D 1970 Dynamic properties of soils and a method for their determination (Stroyizdat L)
[5] Riccardo R B 1974 Teters G A Stability of shells made of composite materials (Ed “Znatie” Riga)
[6] Mittelstedt C Erdmann H Schröder K U 2011 Postbuckling of imperfect rectangular composite plates under inplane shear closed-form approximate solutions *Arch Appl Mech*. https://doi.org/10.1007/s00419-010-0491-y.
[7] Bedair O 2009 Analytical effective width equations for limit state design of thin plates under non-homogeneous in-plane loading *Arch Appl Mech* https://doi.org/10.1007/s00419-009-0296-z.
[8] Golmakani M E Sadraee Far M N 2017 Buckling analysis of biaxially compressed double-layered graphene sheets with various boundary conditions based on nonlocal elasticity theory (Microsyst Technol) https://doi.org/10.1007/s00542-016-3053-6.
[9] Ngo N D Tamma K K 2003 Computational developments for simulation based design: Multi-scale physics and flow thermal/cure/stress modeling, analysis, and validation for advanced manufacturing of composites with complex microstructures https://doi.org/10.1007/BF02736208.
[10] Narendar S 2012 Gopalakrishnan S Scale effects on buckling analysis of orthotropic nanoplates based on nonlocal two-variable refined plate theory *Acta Mech*. https://doi.org/10.1007/s00707-011-0560-5.
[11] Yuan X Guo K 2015 Modelling and analysis for a pilot relief valve using CFD method and deformation theory of thin plates *Sci China Technol Sci* https://doi.org/10.1007/s11431-015-5822-3.
[12] Li Y Liu Y Liu R 2019 Finite Element Analysis on Axial Compressive Behaviors of High-Performance Steel Stiffened Plates in Bridge Application *Int J Steel Struct* https://doi.org/10.1007/s13296-019-00238-y.
[13] Shin D K Cho E Y Kim K 2013 Ultimate flexural strengths of plate girders subjected to web local buckling *Int J Steel Struct* https://doi.org/10.1007/s13296-013-2008-3.
[14] Nakhatakyan F G 2011 Solution of a plane contact problem of the theory of elasticity on the

basis of an elastic half-space model *J Mach Manuf Reliab* https://doi.org/10.3103/S1052618811050141.

[15] Rabnov Y N 1966 Long-term stability of plates and shells *Mech Polym* **2** pp 314–318

[16] Khodzhaev D A Abdikarimov R A Mirsaidov M M 2019 Dynamics of a physically nonlinear viscoelastic cylindrical shell with a concentrated mass *Mag Civ Eng* https://doi.org/10.18720/MCE.91.4.

[17] Usarov M K 2015 Buckling of orthotropic plates with bimoments *Mag Civ Eng* https://doi.org/10.5862/MCE.53.8.

[18] Mirziyod M Ibrokhimovich S I Khudoyberdievich T M 2019 Dynamics of Structural-Inhomogeneous Laminate and Shell Mechanical Systems with Point Constraints and Focused Masses Part 2 Statement of the Problem of Forced Oscillations Methods of Solution Computational Algorithm and Numerical Results *J Appl Math Phys* https://doi.org/10.4236/jamp.2019.711182.

[19] Abdikarimov R A Khudayarov B 2014 Dynamic Stability of Viscoelastic Flexible Plates of Variable Stiffness Under Axial Compression *Int Appl Mech* https://doi.org/10.1007/s10778-014-0642-x.

[20] Teshaev M Safarov I I Mirsaidov M 2019 Oscillations of multilayer viscoelastic composite toroidal pipes *J Serbian Soc Comput Mech* https://doi.org/10.24874/jsscm.2019.13.02.08.

[21] Mirsaidov M M Abdikarimov R A Vatin N I Zhgutov V M Khodzhaev D A Normuminov B A 2018 Nonlinear parametric oscillations of viscoelastic plate of variable thickness *Mag Civ Eng* https://doi.org/10.18720/MCE.82.11.

[22] Koltunov M A Mirsaidov M Troyanovskii I E 1978 Transient vibrations of axisymmetric viscoelastic shells *Polym Mech* **14** pp 233–238 https://doi.org/10.1007/BF00857468.